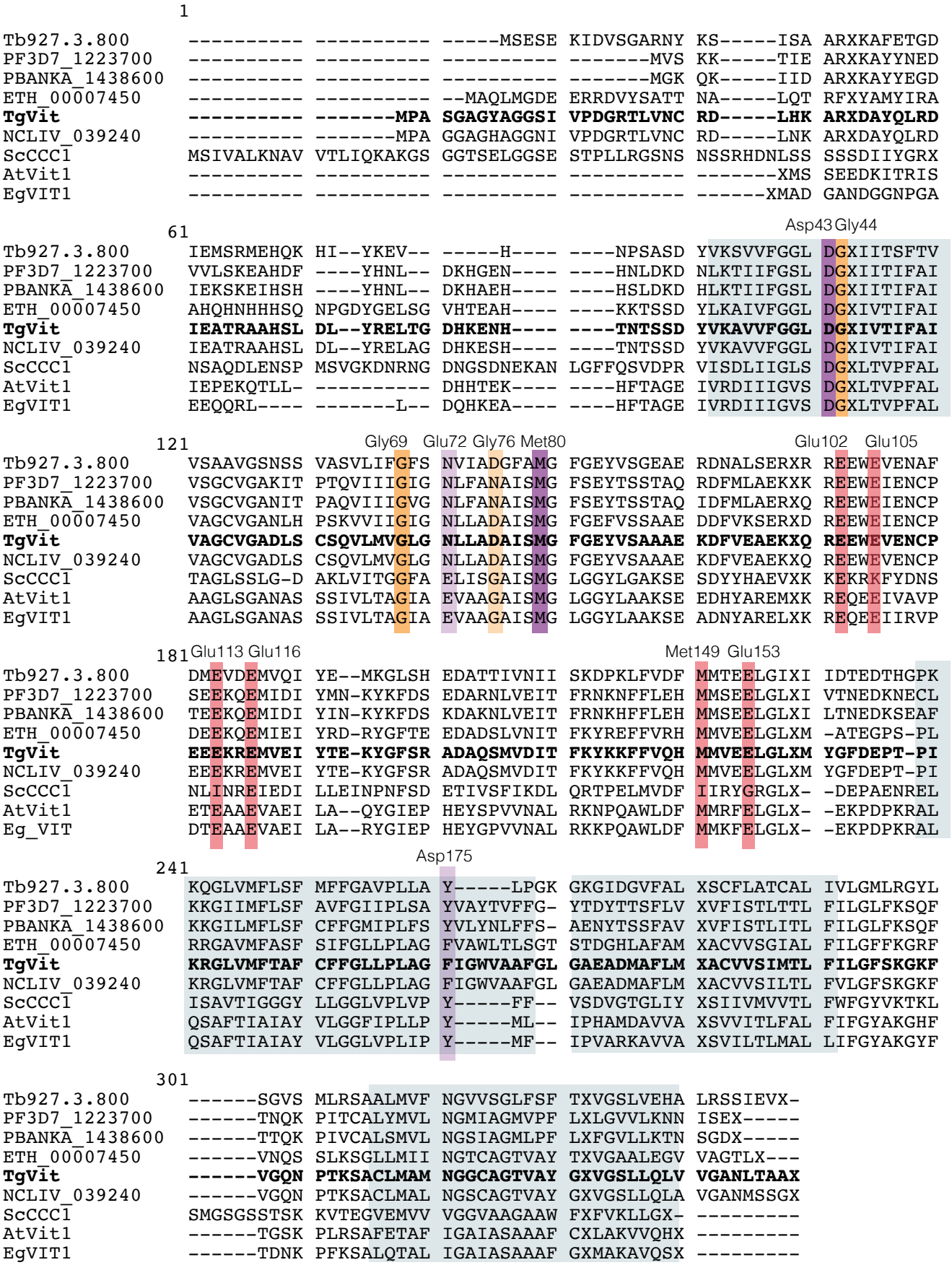

Figure S1. Full alignment of *T. gondii* VIT with VIT sequences from selected eukaryotes. Blue boxes represent transmembrane domains, purple indicates Asp43 and Met80 which are conserved in all VIT members and important for iron binding. Light purple indicates residues important in EgVIT iron binding which are not conserved in apicomplexan sequences. Red indicates conserved residues in the MBD important for Zn coordination. Orange residues indicate conserved 'kink-inducing' residues, important for metal binding the cytoplasmic pocket. All residue numbers from EgVIT.

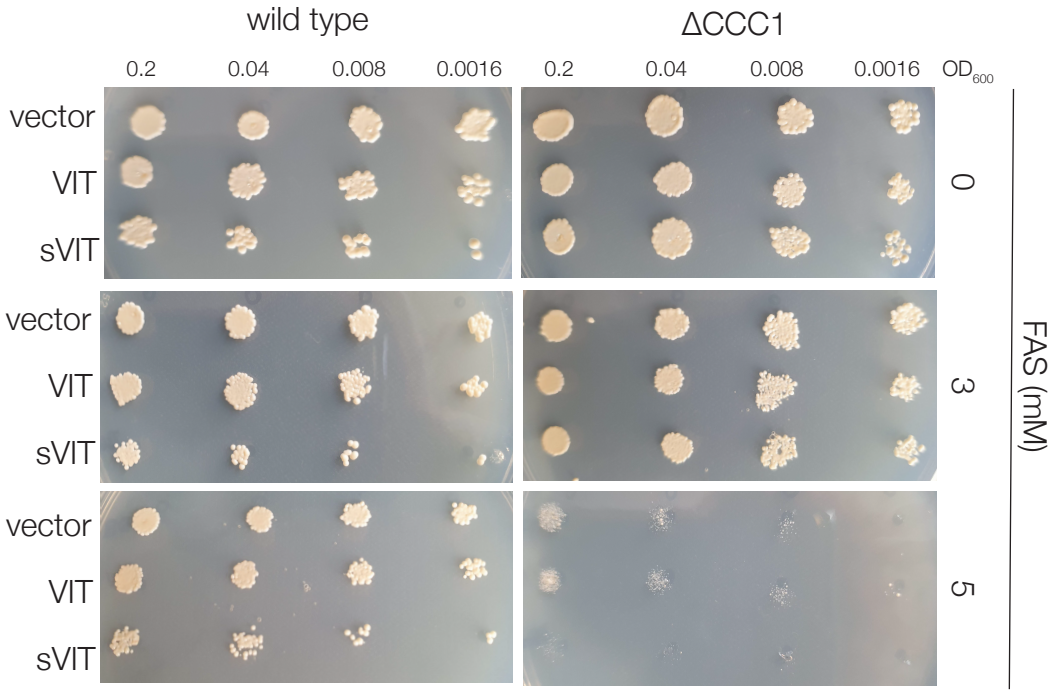

Figure S2. Complementation of yeast with TgVIT. Wild type or ΔCCC1 yeast were transfected with the empty vector or a vector expressing VIT or $sVIT_{63-313}$ (an N-terminal truncation) and plated at the indicated OD_{600} dilution . While the ΔCCC1 strain behaved as expected and was unable to grow on plates containing high iron, expression of VIT or $sVIT_{63-313}$ did not complement the phenotype.

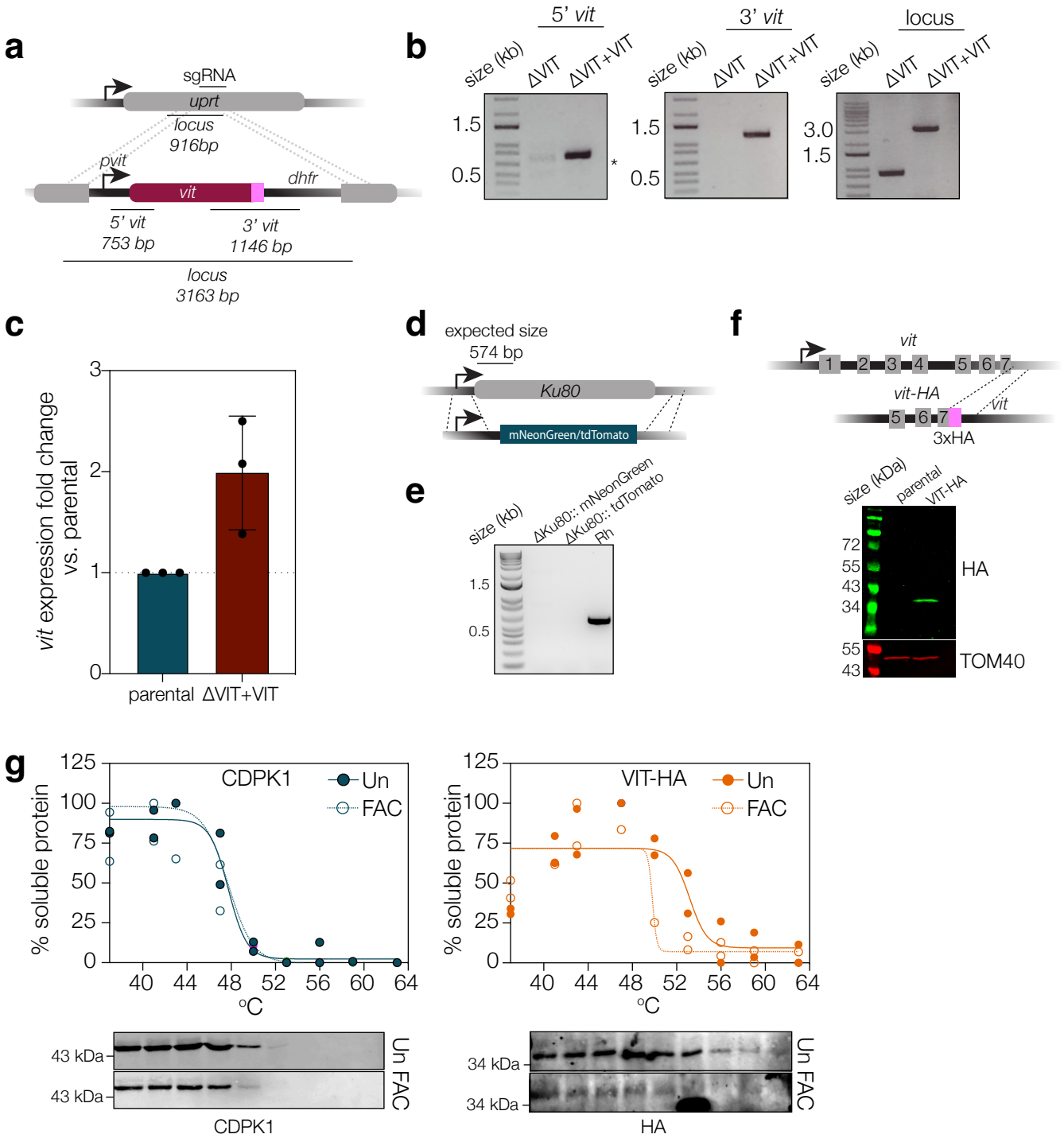

Figure S3. Complementation of ΔVIT parasite line and creation of new ΔKu80 lines expressing mNeonGreen or tdTomato a. Schematic indicating the strategy used to replace the uprt gene with the pvit-vit-3'dhfr cassette. **b.** PCR confirmation of the presence of the vit complementation cassette and the disruption of the endogenous locus, expected sizes indicated in (**a**). Non-specific band marked with asterisk. **c.** qPCR of *vit* in the complemented line shows approximately double the expression compared to parental line. Results are mean ± SD from three independent experiments. Schematic indicating the strategy for replacement of *ku80* gene by mNeonGreen or tdTomato cassettes. **e.** PCR of region indicated in (**d**), confirming the loss of the endogenous gene. **f.** VIT was endogenously tagged at the C-terminal with 3xHA tags. A single band at the expected size (35 kDa) was obtained. **g**. Lysates of VIT-HA parasites treated or untreated for 1 h with FAC were subjected to a range of temperatures as indicated and western blots using anti-CDPK1 and anti-HA performed. Band density plotted, normalised to 37 °C samples, points from two independent experiments.

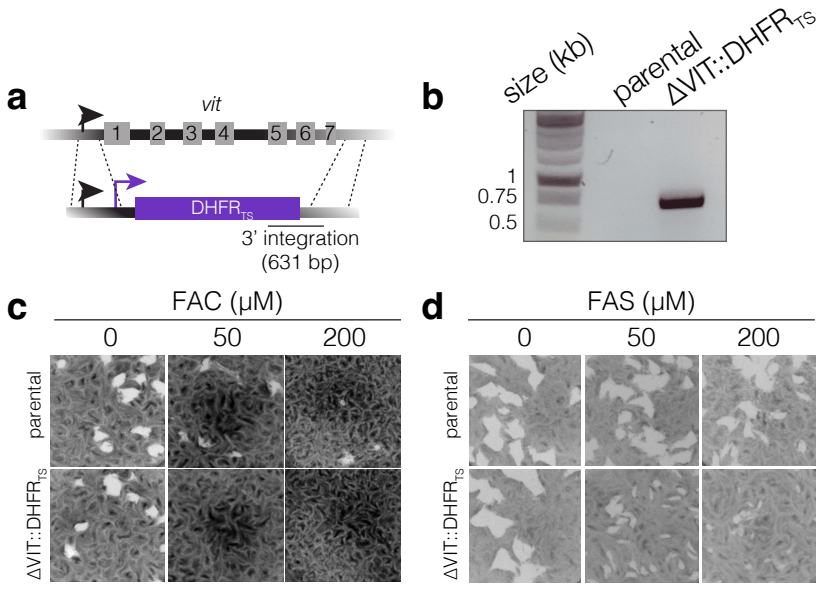

Figure S4. Construction of ΔVIT::DHFRTS parasite line. **a**. Schematic showing how *vit* was replaced with the DHFR cassette. **b.** PCR showing the 5' integration of the DHFR cassette. Plaque assays showing increased sensitivity of the ΔVIT::DHFR$_{TS}$ line to excess ferric ammonium citrate (FAC) **(c)** and ferrous ammonium sulphate (FAS) **(d)** at the indicated concentration compared to the parental parasite line. Representative plaque assays from three independent replicates.

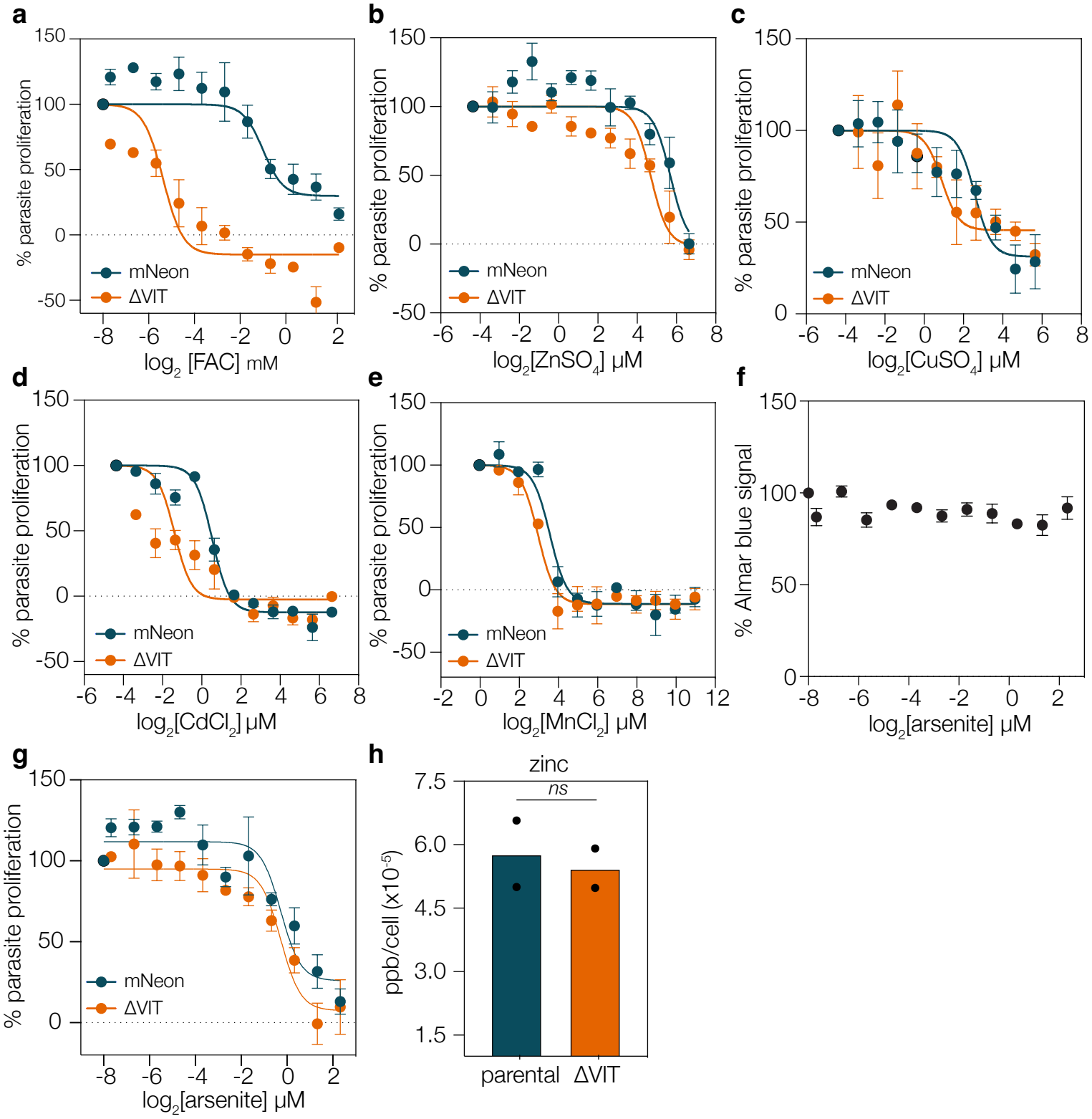

Figure S5. Dose response curves of mNeon and ΔVIT treated with excess metals. As described above, parasites were treated with the indicated concentration of FAC (**a**) $ZnSO_4$ (**b**), $CuSO_4$(**c**), $CdCl_2$(**d**), or $MnCl_2$ (**e**). All experiments are the mean of six (FAC) four ($ZnSO_4$) or three ($CuSO_4$, $CdCl_2$, and $MnCl_2$) independent experiments performed in triplicate, ± SEM. **f.** Survival of uninfected HFF cells at the range of sodium arsenite concentrations used above. No change in fluorescence was seen at the concentrations used. Results are the mean n = 3 independent bioloical replicates, ± SEM. **g.** Treatment of mNeon and ΔVIT parasites with sodium arsenite, a ROS generator, showed no difference in sensitivity between the two lines. Points are the mean of n = 3 independent bioloical replicates, ± SEM. **h.** ICP-MS quantifying zinc (^{66}Zn) from parental and ΔVIT parasites. Each point represents an independent biological replicate, performed in technical duplicate. Bars at mean.

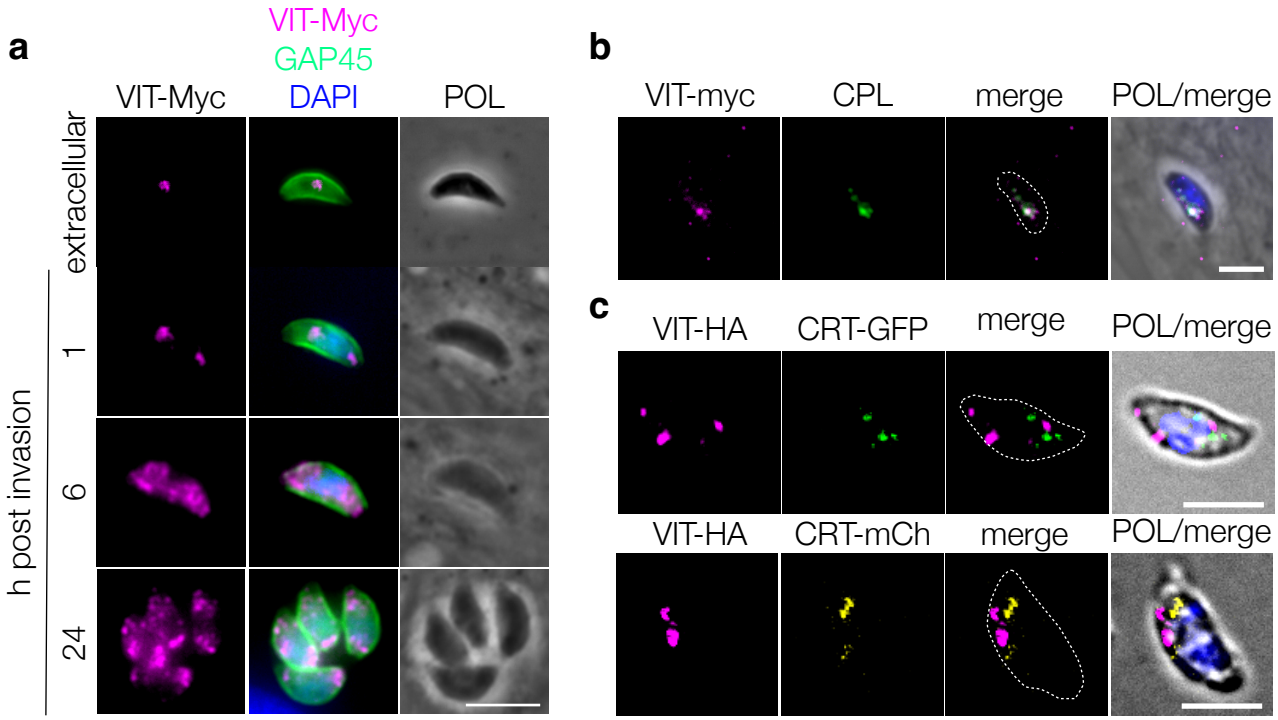

Figure S6. VIT-myc has a dynamic localisation. a. VIT-myc demonstrates a dynamic localisation throughout the cell cycle and fragments between 1 and 6 h post invasion. Cell periphery indicated by GAP45. Representative of three independent experiments. **b.** VIT-myc colocalizes with CPL in extracellular parasites. Representative of two independent experiments. **c.** VIT-HA does not colocalize with transiently overexpressed CRT-GFP or CRT-mCherry in extracellular parasites. Representative of one experiment. Scale bar 5 µm.

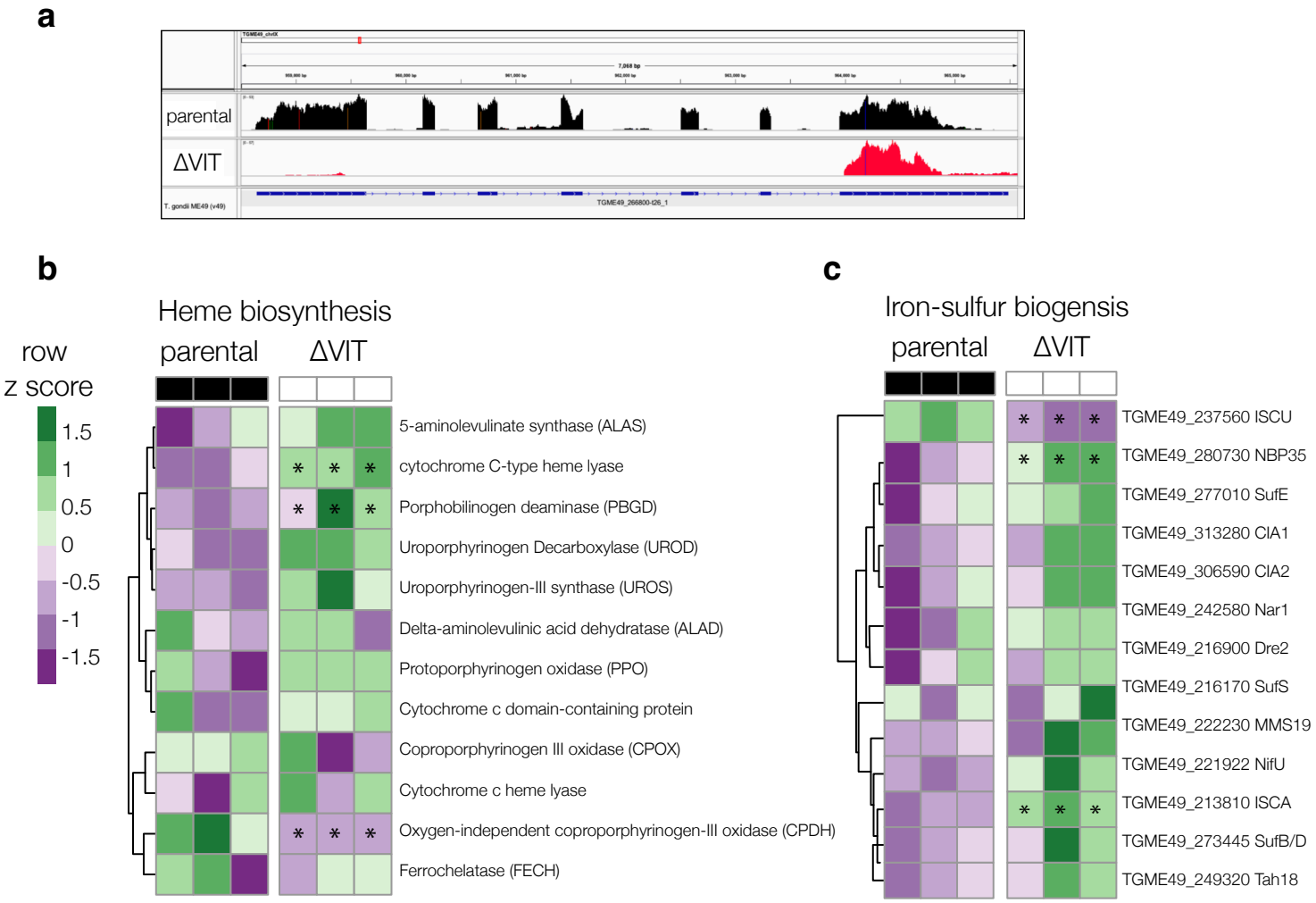

Figure S7. Heatmaps of genes from major iron pathways from parental and ΔVIT parasites a. Mapping of all reads from the parental and ΔVIT strains to the vit gene. As the 5' UTR of *vit* still exists, some reads map to this region, but no reads map to the coding regions**. b**. Genes involved in the heme biosynthesis pathway, read counts normalised across rows. * indicates adj. p value of < 0.05 between parental and ΔVIT strain. **c.** Genes involved in Fe-S biogenesis read counts, normalised across rows. * indicates adj. *p* value from Wald test with Benjamini and Hochberg correction of < 0.05 between parental and ΔVIT strain.

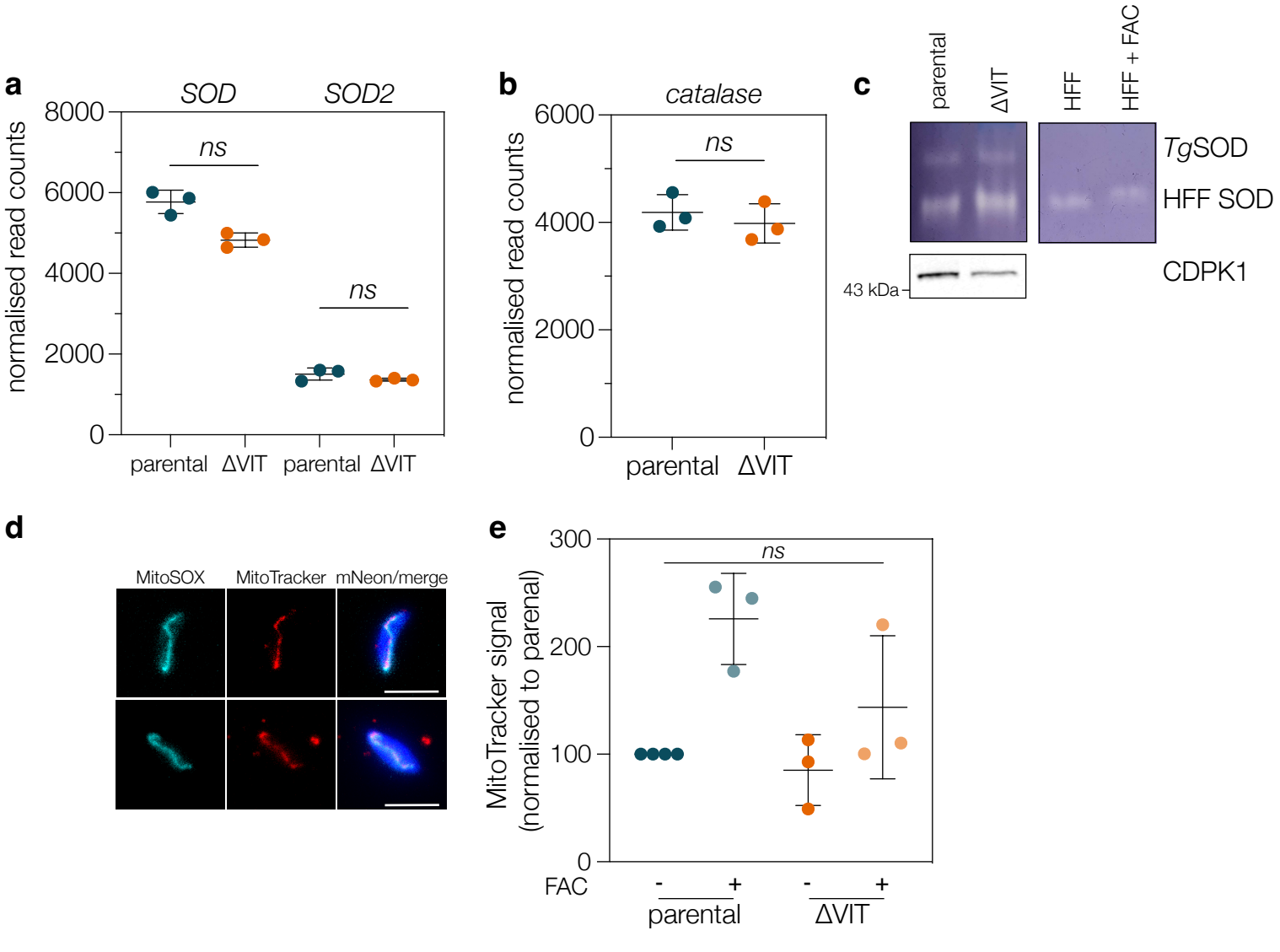

Figure S8. ΔVIT parasites do not alter transcription of oxidative stress genes a. Normalised read counts for *SOD* (TGME49_316310) and *SOD2* (TGME49_316330) from RNAseq. Each point represents an independent experiment, performed in duplicate. Line at mean ± SD. *ns*-non significant from Wald test with Benjamini and Hochberg correction. **b.** Normalised read counts for catalase (TGME49_232250). Each point represents an independent experiment, performed in duplicate. Line at mean ± SD. *p* value from Wald test with Benjamini and Hochberg correction . **c**. In gel activity assay for SOD, enzyme activity results in cleared areas on native gel. Host (HFF) and parasite enzymes indicated, CDPK used as a parasite loading control. No obvious differences were seen between the parental and ΔVIT parasite lines. Results representative of two independent experiments. **d.** Live mNeon parasites were co-stained with MitoSOX Red (cyan) and Mitotracker DeepRed (red) and imaged. MitoSOX and MitoTracker signals co-localised in the mitochondrion of the parasites. Scale bar 5 µm. **e**. MitoTracker signal was measured by flow cytometry and normalised to the mNeon untreated line. Although FAC treatment led to generally increased signal, no significant differences were seen (Kruskal-Wallis test, Dunns multiple comparison correction). Each point represents an independent experiment, $n = 3$, line at mean ± SD.

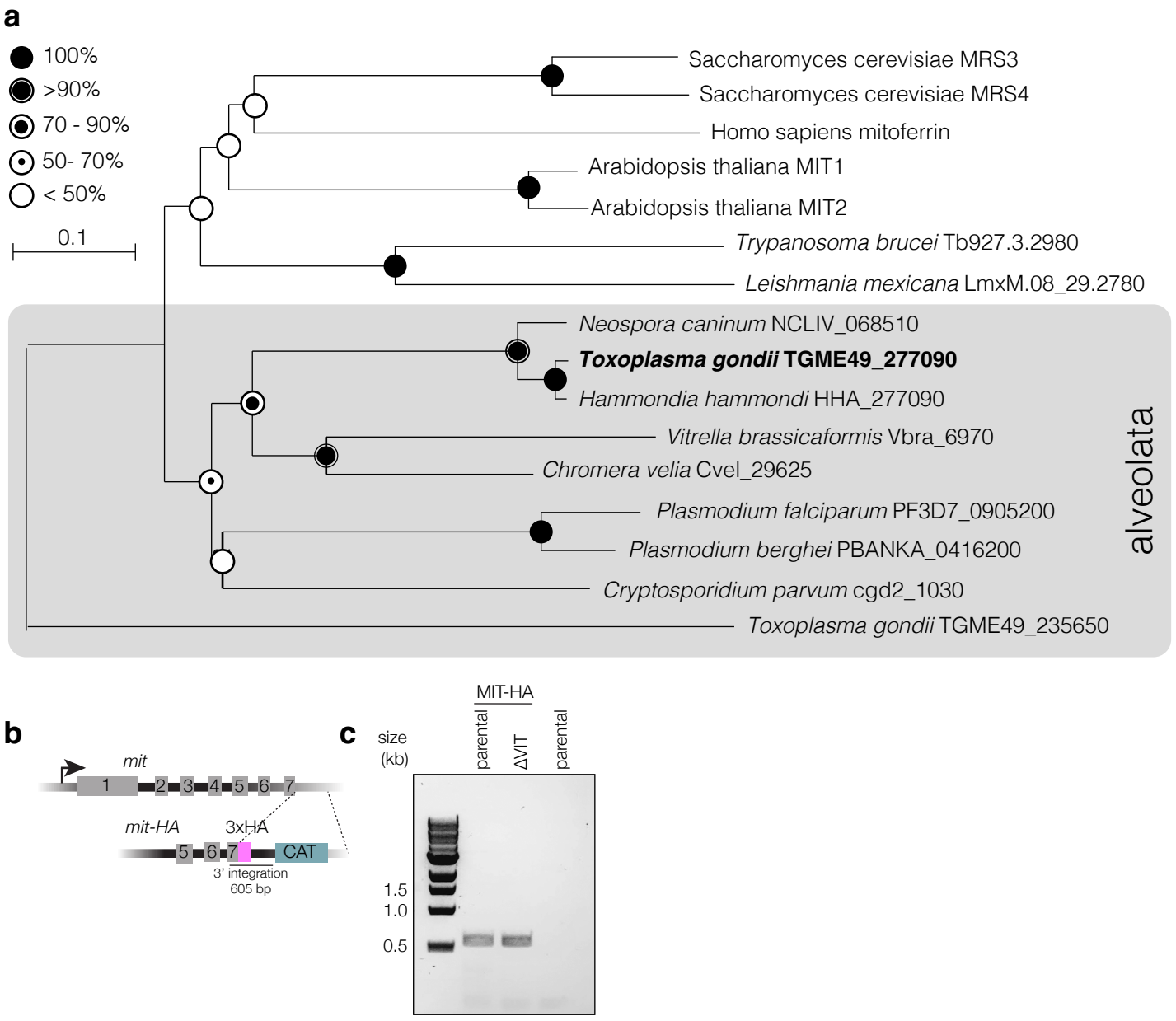

Figure S9. Identification and characterisation of *T. gondii* mitochondrial iron transporter (MIT). a. Phylogenetic tree of MIT sequences from a variety of species. TGME49_235650 represents an unrelated mitochondrial solute carrier. Bootstraps determined from 100 simulations. Scale indicates substitutions per site. **b**. Diagram demonstrating C-terminal HA endogenous tagging strategy. **c.** PCR confirming the integration of HA into MIT locus in the parental (Δku80) and ΔVIT parasite lines.

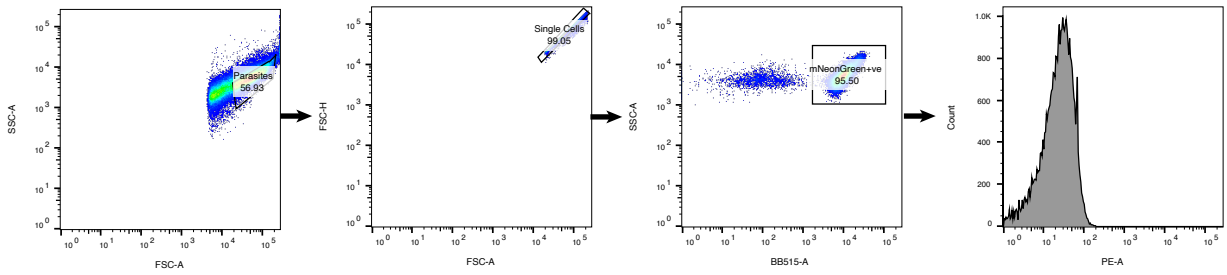

Figure S10. Example gating strategy Δku80::mNeonGreen parasites were stained with MitoSOX as described. Gates were drawn as indicated to isolate parasites, remove doublets and select only mNeonGreen parasites to calculate geometric MFI.